NIH Public Access
Author Manuscript
Biomaterials. Author manuscript; available in PMC 2014 April 01.

Published in final edited form as:
Biomaterials. 2013 April ; 34(12): 2960–2968. doi:10.1016/j.biomaterials.2013.01.058.

Sustained volume retention *in vivo* with adipocyte and lipoaspirate seeded silk scaffolds

Evangelia Bellas[a], **Bruce J.B. Panilaitis**[a], **Dean L. Glettig**[a], **Carl A. Kirker-Head**[b], **James J. Yoo**[c], **Kacey G. Marra**[d], **J. Peter Rubin**[d], and **David L. Kaplan**[a,*]

[a]Biomedical Engineering, Tufts University, Medford, MA 02155, USA

[b]Cummings School of Veterinary Medicine, Tufts University, N. Grafton, MA 01536, USA

[c]Wake Forest Institute for Regenerative Medicine, Winston-Salem, NC 27157, USA

[d]Department of Surgery, University of Pittsburgh, Pittsburgh, PA 15213, USA

Abstract

Current approaches to soft tissue regeneration include the use of fat grafts, natural or synthetic biomaterials as filler materials. Fat grafts and natural biomaterials resorb too quickly to maintain tissue regeneration, while synthetic materials do not degrade or regenerate tissue. Here, we present a simple approach to volume stable filling of soft tissue defects. In this study, we combined lipoaspirate with a silk protein matrix in a subcutaneous rat model. Silk biomaterials can be tailored to fit a variety of needs, and here were processed silk biomaterials into a porous sponge format to allow for tissue ingrowth while remaining mechanically robust. Over an 18 month period, the lipoaspirate seeded silk protein matrix regenerated subcutaneous adipose tissue while maintaining the original implanted volume. A silk protein matrix alone was not sufficient to regenerate adipose tissue, but yielded a fibrous tissue, although implanted volume was maintained. This work presents a significant improvement to the standard approaches to filling soft tissue defects by matching biomaterial degradation and tissue regeneration profiles.

Keywords

Adipose tissue engineering; *In vivo* test; Protein; Scaffold; Silk; Stem cell

1. Introduction

Soft tissue defects result from congenital abnormalities, trauma, or tumor resections [1]. They constitute about 4.8 million reconstructive surgery cases per year in the US (www.plasticsurgery.org). These defects can carry emotional and social consequences associated with deformity. Autografts have been widely explored for soft tissue reconstruction, however, fat grafting, as with other natural and synthetic biomaterial fillers, does not retain volume over time, with 20–90% of the filler volume lost over the first few months [2,3].

© 2013 Elsevier Ltd. All rights reserved.

*Corresponding author. Fax: +1 617 627 3231. David.Kaplan@tufts.edu (D.L. Kaplan).

Appendix. Supplementary data

Supplementary data related to this article can be found at http://dx.doi.org/10.1016/j.biomaterials.2013.01.058.

NIH-PA Author Manuscript
NIH-PA Author Manuscript
NIH-PA Author Manuscript

NIH-PA Author Manuscript

NIH-PA Author Manuscript

NIH-PA Author Manuscript

Loss of volume is the result of avascular necrosis and adipocyte delipidation. Avascular necrosis occurs when the volume of tissue implanted does not become fully vascularized in a timeframe to support the metabolic needs of the tissue. Adipocyte delipidation ensues from mechanical disruption during the transfer and also when the adipocytes become apoptotic. For these reasons, this leaves significant problems for patients thus regeneration of soft tissue defects remains an unmet need. In 1951, Peer and Walker reported on the outcome of 28 human fat grafts and found that 50% of the transplanted tissue remained after 1 year, whether it was placed near a vascular supply or a like tissue, such as muscle [4,5]. Like tissue, in this case, was defined as another highly cellular tissue, in contrast to a tissue like bone or tendon which is rich in extracellular matrix. The adipocytes that did not survive were replaced with fibrotic tissue. More recently, studies have shown that during the process of liposuction and preparation of the lipoaspirate for lipotransfer that some of the regenerative aspects are lost [6,7]. This is believed to be the result of the lack of adipose derived stem cells (ASCs) within the lipoaspirate. The ASCs were found to reside near the vasculature in subcutaneous adipose tissue and are often left anchored to the vasculature as the other parts of the adipose tissue are aspirated. ASCs in this capacity are thought to serve as pericytes (the supporting cells in the microvasculature), differentiate into endothelial cells or play a role in adipose tissue turnover by differentiating into adipocytes. When lipotransfer was enriched with additional ASCs the implanted tissue was better able to maintain its original volume in *in vivo* studies, however no volume maintenance was reported for the human clinical studies.

Several adipose tissue engineering approaches with various cell sources and both artificial and natural biomaterials have been studied *in vivo* [8]. Many of these studies failed to maintain volume or regenerate adipose tissue over an extended timeframe. A few reported long-term results, but had initially formed an adipose tissue mound grown in a vascular rich environment, such as within muscle, and then transferred the tissue to another site [9,10]. Although promising, this method requires multiple surgical sites and various staggered operative days since the tissue needs to be cultured elsewhere for a period of time and then excised and transferred to the site of interest. Therefore, for the restoration of traumatic soft tissue defects, the maintenance of tissue size and shape to near-normal dimensions for extended timeframes is critical to avoid subsequent repeated treatments or surgeries and to maintain a specific esthetic. The construct must be maintained *in vivo* as the body gradually remodels and regenerates the site into near-normal tissue structure and function.

Silk, a protein biomaterial, has been used extensively for sutures [11,12] and recently FDA approved as a surgical mesh, can be processed into a variety of formats with predetermined degradation rates [13]. We have previously demonstrated silk matrices support adipogenesis both *in vitro* and *in vivo* [14,15]. Silk porous sponges were also shown to last over 1 year *in vivo* in a rat model [16]. The degradation rate of silk biomaterials is controlled by varying the degree of protein crystallinity during processing, reflecting the physical beta sheet crosslinks, thus no chemical crosslinking is required. In this study, the objective was to assess whether the combination of mechanically robust, porous silk sponges designed to degrade slowly *in vivo* along with a biological component, human ASCs or lipoaspirate, could foster volume maintenance and soft tissue regeneration over an extended timeframe.

2. Methods and materials

Bombyx mori silkworm cocoons were supplied by Tajima Shoji Co. (Yokohama, Japan). All cell culture supplies and collagenase type I were purchased from Invitrogen (Carlsbad, CA) unless otherwise noted. Human recombinant insulin, dexamethasone, pantothenate, biotin, 2,3-thiazolidinediones (TZD), 3-isobutyl-1-methylxanthine (IBMX), bovine serum albumin (BSA), and laminin from human placenta were also purchased from SigmaeAldrich (St.

NIH-PA Author Manuscript

NIH-PA Author Manuscript

NIH-PA Author Manuscript

Louis, MO). Histological solvents were purchased from Fisher Scientific (Pittsburgh, PA) and histological reagents and Masson's Trichrome Stains Kit were purchased from Sigma–Aldrich.

2.1. Silk sponge preparation

Silk solution was prepared as published [17]. The aqueous silk solution was lyophilized until dry and re-solubilized over 2 days in hexafluoro-2-propanol (HFIP) at 17% w/v. Salt crystals were sieved to the desired range of 500–600 μm, poured into Teflon coated petri dishes and either aqueous silk or HFIP-silk solution was added. The Petri dish was covered and left in a fume hood for 2 days and, uncovered to let the HFIP evaporate for 1 day. The dish was immersed in methanol overnight, left in the fume hood for 1 day for the methanol to evaporate and then placed in water to leach out the salt particles. The water was changed 3 times a day for 2 days. The sponges were removed from the petri dish, cut to the desired dimension, 5 mm diameter × 2 mm height, using a biopsy punch. The sponges were left to dry before autoclaving, autoclaved, then kept at 4 °C until use. The sterile sponges were first rehydrated in phosphate buffered saline (PBS), and then dip-coated twice in 10 μg/ mL sterile solutions of laminin for 15 min and let to dry.

2.2. Human adipose derived stem cell isolation

Subcutaneous adipose tissue was obtained from abdominoplasties under Tufts University IRB (Tufts University IRB Protocol #0906007) from the Tufts Medical Center, Department of Plastic Surgery. The specimens were kept at room temperature in saline and used within the same day. The adipose tissue was separated from the skin by blunt dissection and chopped. Chopped adipose tissue was placed into 50 mL conical tubes and minced well with scissors. The tissues were washed in equal volumes warmed PBS, until essentially free of blood. An equal volume of 1 mg/mL collagenase I in 1% bovine serum albumin in PBS was added to the tissue and placed under gentle agitation at 37 °C for 1 h. The tissue samples were centrifuged at 300 × *g* for 10 min at room temperature. The supernatant containing the tissue was removed and the pellet re-suspended in PBS and centrifuged at the same settings to remove the collagenase solution. The pellet was re-suspended in growth media and plated so that 70 g of initial tissue volume was plated per T225 cm^2 tissue culture flask.

2.3. Cell culture and 3D culture

Adipose derived stem cells were expanded and cultured as previously described [14,18]. Cells were expanded first in growth media comprised of DMEM/F12, 10% fetal bovine serum (FBS), 1% penicillin–streptomycin–fungizone (PSF) until confluence. At 2 days post-confluence, the cells were switched to adipogenic induction media comprised of DMEM/F12, 3% FBS, 1% PSF, 500 μM IBMX, 5 μM TZD, 1 μM dexamethasone, 17 μM pantothenate, 33 mM biotin and 1 μM insulin for 1 week. The dry, coated sponges were placed into adipogenic maintenance media for 1 h before seeding with cells. Maintenance media was identical to induction media but without IMBX and TZD. The induced ASCs were detached with trypsin and re-suspended in maintenance media at a density of 3,333,333 cells/mL. Cells were seeded in 3 × 20 μL seedings with a total of 200,000 cells/sponge. The seeded sponges were placed in an incubator for 2 h before media was added to the well. Cells and cultures were fed 2 times per week, and maintained in 37 °C, 5% CO_2 humidified incubator.

2.4. Lipoaspirate seeding

Lipoaspirate from elective plastic surgery was obtained the same day of sponge implantation. Lipoaspirate was transported aseptically at room temperature just after surgery. Approximately 30 mL of lipoaspirate was added to a 50 mL conical tube and centrifuged at room temperature at 1000 rpm for 10 min. The blood and free lipids were

NIH-PA Author Manuscript

NIH-PA Author Manuscript

NIH-PA Author Manuscript

removed. The remaining tissue was placed in sterile petri dishes. The dry, silk sponges were placed into the processed lipoaspirate for 1 h prior to implantation.

2.5. In vivo implantation

Animals were cared for in compliance with Tufts University Institutional Animal Care and Use Committee (IACUC) in accordance with the Office of Laboratory Animal Welfare (OLAW) at the National Institutes of Health (NIH). Adult, male athymic T-cell deficient RH-rnu rats (9 weeks old) were purchased from Taconic Farms (Cambridge City, Indiana) and were allowed to acclimate for 1 week prior to implantation. The rats were randomly assigned to one of the three implant groups. The animals were first anesthetized with isoflurane (1–4%) and then administered the following analgesic, anti-inflammatory, antibiotic cocktail: carprofen, 5 mg/kg subcutaneously, buprenorphine, 0.05 mg/kg subcutaneously, and procaine penicillin, 200,000 IU/kg intramuscularly. The animals were maintained with 1% (or to effect) isoflurane in oxygen, and kept on a heating pad through the entire procedure. After induction of anesthesia, the surgical site was clipped with electrical clippers. The skin was then aseptically prepared with chlorohexidine scrub followed by an alcohol rinse, repeated three times. A small skin incision (~7 mm) was made between the shoulder blades, and 2 tunnels were formed under the skin by blunt dissection along either side of the spine, 5–8 cm away from the initial skin incision. The implants were placed above the underlying muscle under the skin at the end of the tunneled area. The skin was stapled at the incision site. The animals were allowed to awaken and had free access to food and water, thereafter.

2.6. Histology

Constructs were processed according standard histology protocols. Formalin fixed samples were put through a series of dehydration solvents and finally paraffin using an automated tissue processor. Samples were embedded in paraffin, cut in 10 μm sections, and let to adhere on glass slides. The sections were rehydrated and stained with Hematoxylin and Eosin (H&E) for general morphology and organization, Masson's Trichrome for tissue remodeling, Prussian Blue Test for iron staining. To evaluate lipid accumulation, the formalin fixed constructs were embedded in OCT (Optimal Cutting Temperature) compound medium and frozen. The frozen blocks were cut in 10 μm sections, and then stained with Oil Red O.

2.7. Scanning electron microscopy imaging

Explanted implants with surrounding tissue were frozen at −80 °C until ready to process for imaging. Explants were washed in 0.1 M phosphate buffer, and then fixed in freshly prepared 2.5% glutaraldehyde in 0.1 M phosphate buffer for 1 h. The explants were washed in phosphate buffer, and then fixed in osmium tetroxide in 0.1 M phosphate buffer for 1 h. The explants were dehydrated in a graded ethanol series, starting at 50% ethanol until dehydrated at 100% ethanol. Hexamethyldisilazane (HMDS) was added to the explants, removed, and then the explants were placed in a desiccator overnight. The dried explants were sputter coated (208HR Sputter-Coater, Cressington Scientific Instruments Ltd., Walford, England) with platinum for 1 min. Pt-coated explants were imaged by SEM (Supra55VP, Carl Zeiss Nano Technology Systems, Peabody, MA).

2.8. Tissue regeneration measurements

During implant harvest, subcutaneous tissue layers, with the included implant, were carefully dissected away from the underlying muscle. The implants were cut out with the surrounding skin and tissue intact. The implant was then cut along its diameter to expose its cross-section and the cross-sections were photographed. Image analysis was carried out

NIH-PA Author Manuscript

NIH-PA Author Manuscript

NIH-PA Author Manuscript

using ImageJ software (U.S. National Institutes of Health, Bethesda, Maryland, USA). Images of implant cross-sections were cropped to the region of interest and converted to 8-bit images. Contrast was enhanced and the image was sharpened (default settings used for both). This allowed for enhanced discrimination between the tissue and the silk sponge. The height/thickness of the surrounding subcutaneous fat was measured 3 times along the cross-section with the straight line tool, and the 3 measurements were averaged. This same procedure was used to determine the height/thickness of the silk sponge. The average of the silk sponge was subtracted from the subcutaneous fat, to yield an approximated value of regenerated tissue. The average height/thickness values for both regenerated tissue and silk sponge were plotted as a function of time and seeding condition.

2.9. Statistical analysis

Samples for all quantifiable analyses were $n = 4–6$ with each biological replicate having technical duplicates. Histological analyses were performed at $n = 3$, with 3 consecutive sections being taken per staining group, only representative images are shown. Results are shown as means ± SD. All statistical analyses were performed on Excel (Microsoft, Redmond, WA).

3. Results

3.1. In vivo observations

The silk sponges seeded with human ASCs and cultured *ex vivo* in adipogenic conditions for 4 weeks formed tissue throughout the entire sponge. The sponges also readily absorbed lipoaspirate (Fig. 1a). Lipoaspirate is the aspirated portion of adipose tissue, comprised of mature adipocytes, ASCs, vascular cells, extracellular matrix proteins, growth factors and cytokines [19,20].

Adult, male athymic T-cell deficient RH-rnu rats were selected for this long-term study to minimize sex hormone effects on adipogenesis and also to permit the use of human cells or tissue without rejection. The constructs were implanted subcutaneously as described in Methods. No acute or chronic adverse reactions were evident and rats continued to gain weight normally over 18 months (Supplementary Fig. 1a). The spleens were assessed at each timepoint for changes but no differences were noted (Supplementary Fig. 1b).

3.2. Macroscopic observations

All sponges were soft to the touch and retained their ability to return to their shape after deformation. At each timepoint small blood vessels were seen surrounding the sponges in the subcutaneous tissue and all groups had integrated with the surrounding tissues (Fig. 1b). Integration, as seen by host tissue infiltration had further improved in the groups that were pre-seeded when compared to the unseeded group (Fig. 1b). At 12 and 18 months, integration with the surrounding tissue was even more evident (Fig. 1c). Blood vessels were seen in all study groups and appeared to be functional based on the presence of red blood cells within the lumens (Fig. 1c).

3.3. Sponge degradation

Sponge volume retention was stable for at least the first 6 months (Fig. 2a). Degradation of the silk sponges was seen in all study groups (Fig. 2a). The lipo-seeded group was completely encased in a fat pocket by 12 months and still apparent out to 18 months (Fig. 2b). We approximated the thickness of the newly formed tissue by measuring the thickness of the subcutaneous fat and subtracting the thickness of the silk sponge. The total thickness (sponge and regenerated tissue) was maintained over the 18 month period in all groups (Fig. 2c). The unseeded sponge's structure remained intact with open pores and tissue infiltration

NIH-PA Author Manuscript

NIH-PA Author Manuscript

NIH-PA Author Manuscript

(Fig. 3). No changes were seen in pore wall thickness or overall sponge structure when explanted implant cross-sections were assessed by SEM (Fig. 3), suggesting degradation occurs from the outer boundaries of the sponge inward.

3.4. Histological observations at 3 and 6 months

Histological images at 3 months show silk sponges were present in all groups (Fig. 4). Some macrophages were evident near the sponges demonstrating dynamic remodeling, as silk degrades via proteolytic action (Fig. 4a) [21]. The unseeded group had the greatest number of macrophages present at 3 months while the lipo-seeded group had the least number of macrophages (Fig. 4a). Macrophages are known to secrete proteolytic enzymes and fibroblast mitogens for tissue repair [22]. The unseeded group showed a poorly organized matrix and less tissue infiltration into pores than the seeded groups, confirming the macroscopic observations (Fig. 4b). Oil Red O (ORO) staining for mature adipocytes was performed and positive staining in the vicinity of the sponge was seen in the seeded study groups (Fig. 4c). In the unseeded group, positive staining for ORO was detected at the interface with the muscle and near the sponges. At 6 months, the silk sponges were evident in all study groups though with fewer macrophages seen than at 3 months. In the unseeded group, the tissue had infiltrated the pores of the sponge, similar to that seen earlier (at 3 months) in the seeded groups (Fig. 4a). Positive staining for ORO was seen in all study groups, including the unseeded group, albeit less intense in staining than in the seeded groups (Fig. 4c). Unlike the seeded groups, positive staining was seen more along the periphery of the unseeded group sponge than within (Fig. 4c).

3.5. Histological observations at 12 and 18 months

The silk sponge structures were still present; however, the pore walls had begun to fracture as they degraded (Fig. 5a, b). The unseeded group had few mature adipocytes present, with most residing at the interface between the implant boundaries and the surrounding tissue (Fig. 5c). The seeded groups contained large, mature adipocytes throughout the constructs (Fig. 5c). ORO staining was seen in all study groups, with denser pockets of staining in the lipo-seeded group than the unseeded or ASC-seeded groups (Fig. 5c). Interestingly, all lipo-seeded groups had prominent blood vessels feeding into the sponges from the underlying *Latissimus dorsi* muscle (Fig. 6), suggesting a large blood supply is necessary to support the mature, regenerated adipose tissue.

4. Discussion

Soft tissue restoration or augmentation has been studied for many years. A common approach to soft tissue restoration is fat grafting but the most challenging aspect of this approach has been volume retention over time due to graft resorption. Volume loss or resorption is caused by many factors: inability of adipocytes to proliferate, adipocyte delipidation or inadequate vascularization [23]. The goal of the present work was to determine a biomaterial/tissue construct that would address this problem, while also being amenable to clinical translation. Porous silk sponges are readily formed to desired shape and porosity, and in the dried state these sponges can be autoclaved and stored aseptically at room temperature for years until needed. When these protein sponges were hydrated they were soft and spongy and able to be deformed, returning to their original dimensions immediately after the release of the applied pressure.

The initial sponge volume did not decrease because the silk sponges maintained structure during the tissue remodeling process. Silk biomaterials were chosen based on their ability to be tailored to fit a wide range of mechanical and degradation profile, as well as being unlimited in terms of total sponge size and shape. We have previously demonstrated that silk

NIH-PA Author Manuscript

NIH-PA Author Manuscript

NIH-PA Author Manuscript

sponge biomaterials can be processed to last more than 12 months *in vivo* in a rat model [16], or be immediately resorbed [17,24]. We have also demonstrated that silk biomaterials can be useful in support of adipose tissue engineering *in vitro* and *in vivo* [14,15]. Other natural biomaterials, such as collagen and hyaluronic acid, degrade quickly unless crosslinked. Even when cross-linked, degradation remains relatively rapid when compared to silk biomaterials [25,26]. Silk requires no crosslinking due to the extensive network of physical crosslinks in the form of beta sheets. Due to these secondary structures, silk as prepared in the present study will not contract or swell significantly, which is a common challenge with other polymeric degradable biomaterials. This maintenance of structure of a very slowly degrading biomaterial allowed tissue regeneration and sustained biological function during the remodeling process, without the loss of implant volume. This represents a major advance over current biomaterial options used for soft tissue regeneration. The remodeling process continued within the sponge structure due to the maintenance of mass transport by keeping the porous structure open. By the time the sponges began to degrade at 12 months, tissue formation in all study groups had been well established, complete with vasculature. In all cases, the sponges began degrading from the outside inward. This was evident in SEM images where the pore wall thickness did not change significantly over time and the aspect ratio of the cylindrical implant remained intact. The surrounding host fibroblasts and macrophages secrete non-specific proteases to slowly break down the silk sponges [16,22].

Animal studies have been carried out in both immunodeficient and nonimmunodeficient strains [8]. It is well-accepted immunodeficient strains, such as the one used in this study have different wound healing kinetics, yet their use was deemed necessary for implantation of human cells and tissue. Similarly, studies should be compared only to matched strains due to differences in metabolic profiles between strains, possibly biasing some strains to enhanced adipogenesis [8]. Our group had previously compared silk sponges implanted intramuscularly in immunodeficient and nonimmunodeficient strains of rats and found that aqueous processed silk sponges degraded more quickly in nonimmunodeficient rats [16]. However, the degradation rate in HFIP processed silk sponges, like the sponges in this study, was not affected by immune state and appeared more resistant to macrophage mediated degradation than aqueous processed silk sponges [16].

Animal studies to study soft tissue reconstruction and regeneration are generally run over a relatively short term (~8 weeks) [8]. To our knowledge, no prior study has shown greater than 6 months volume maintenance for soft tissue regeneration. Two other studies in rats have demonstrated long-term retention out to 12 months [9,10], however these studies used pedicle flaps which were implanted in another part of the body, allowed to become vascularized and then transplanted to the site of interest. This method is less desirable than our current approach due to the large mass that will need to be harvested from a donor site, as well as the need for multiple surgeries and thereby multiple morbidity sites. The method presented here only requires a minimally invasive procedure, liposuction, to harvest the lipoaspirate or ASCs.

In the present study, silk porous proteins sponges, alone, or seeded with *in vitro* differentiated human ASCs or freshly isolated lipoaspirate, were implanted into nude rats. The harvest of lipoaspirate is already clinically used for fat grafting. The isolation of ASCs from lipoaspirate could be performed in the clinic using rapid and automated procedures, such as the TGI System (Tissue Genesis, Inc., Honolulu, HI). We chose to compare freshly isolated lipoaspirate to *in vitro* differentiated ASCs cultured for 4 weeks on the sponges, as the lipoaspirate contains active vascular growth factors that may enhance tissue regeneration [19,27]. Fresh ASCs have been postulated to take on a perivascular phenotype [28]. Further, harvesting and processing lipoaspirate can be done the same day as the implantation without

NIH-PA Author Manuscript

NIH-PA Author Manuscript

NIH-PA Author Manuscript

scarring, and no *ex vivo* manipulation that would require FDA approval is needed to re-implant the lipoaspirate.

5. Conclusions

We successfully demonstrate complete retention of volume for more than 6 months following implantation of soft tissue regeneration systems in a small animal model. At 12–18 months the sponges began degrading while encased in their own fat pockets, thus tissue regeneration without significant loss of volume. The histological changes over time support the conclusion that the silk porous sponges acted as templates for dynamic tissue regeneration even during this remodeling process. These results point toward a viable clinical strategy to address this major surgical need for soft tissue regeneration.

Supplementary Material

Refer to Web version on PubMed Central for supplementary material.

Acknowledgments

The authors wish to acknowledge Eun Seok Gil, Jelena Rnyak, Rebecca S. Hayden and David Lange for their assistance with SEM preparation and imaging, Ethan Golden for histopathological insight. They also wish to thank Dr. Daniel Driscoll for providing surgical specimens, Marianne Stark and Kimberly Flink for assistance with surgeries and animal care. The SEM work was performed in part at the Center for Nanoscale Systems (CNS), a member of the National Nanotechnology Infrastructure Network (NNIN), which is supported by the National Science Foundation under NSF award no. ECS-0335765. CNS is part of Harvard University. This work was funded by Armed Forces Institute for Regenerative Medicine (AFIRM) W81XWH-08-2-0032 and the NIH – P41 EB002520.

References

1. Stosich MS, Moioli EK, Wu JK, Lee CH, Rohde C, Yoursef AM, et al. Bioengineering strategies to generate vascularized soft tissue grafts with sustained shape. Methods. 2009; 47:116–121. [PubMed: 18952179]
2. Patrick C. Tissue engineering strategies for adipose tissue repair. Anat Rec. 2001; 366:361–366. [PubMed: 11500812]
3. Gomillion CT, Burg KJ. Stem cells and adipose tissue engineering. Biomaterials. 2006; 27:6052–6063. [PubMed: 16973213]
4. Peer LA, Walker JC. The behavior of autogenous human tissue grafts; a comparative study. 1. Plast Reconstr Surg. 1951; 7:6–23.
5. Peer LA, Walker JC. The behavior of autogenous human tissue grafts. II. Plast Reconstr Surg. 1951; 7:73–84.
6. Yoshimura K, Sato K, Aoi N, Kurita M, Hirohi T, Harii K. Cell-assisted lipotransfer for cosmetic breast augmentation: supportive use of adiposederived stem/stromal cells. Aesthetic Plast Surg. 2008; 32:48–55. [PubMed: 17763894]
7. Matsumoto D, Sato K, Gonda K, Takaki Y, Shigeura T, Sato T, et al. Cell-assisted lipotransfer: supportive use of human adipose-derived cells for soft tissue augmentation with lipoinjection. Tissue Eng. 2006; 12:3375–3382. [PubMed: 17518674]
8. Patrick C, Uthamanthil R. Animal models for adipose tissue engineering. Tissue Eng. 2008; 14:167–178.
9. Wechselberger G, Russell RC, Neumeister MW, Schoeller T, Piza-Katzer H, Rainer C. Successful transplantation of three tissue-engineered cell types using capsule induction technique and fibrin glue as a delivery vehicle. Plast Reconstr Surg. 2002; 110:123–129. [PubMed: 12087242]
10. Schoeller T, Lille S, Wechselberger G, Otto A, Mowlawi A, Piza-Katzer H. Histomorphologic and volumetric analysis of implanted autologous preadipocyte cultures suspended in fibrin glue: a

NIH-PA Author Manuscript

NIH-PA Author Manuscript

NIH-PA Author Manuscript

potential new source for tissue augmentation. Aesthetic Plast Surg. 2001; 25:57–63. [PubMed: 11322400]

11. Altman G, Diaz F, Jakuba C, Calabro T, Horan R. Silk-based biomaterials. Biomaterials. 2003; 24:401–416. [PubMed: 12423595]
12. Vepari C, Kaplan DL. Silk as a biomaterial. Prog Polym Sci. 2007; 32:991–1007. [PubMed: 19543442]
13. Kim HJ, Kim HS, Matsumoto A, Chin I-J, Jin H-J, Kaplan DL. Processing windows for forming silk fibroin biomaterials into a 3D porous matrix. Aust J Chem. 2005; 58:716–720.
14. Kang JH, Gimble JM, Kaplan DL. In vitro 3D model for human vascularized adipose tissue. Tissue Eng Part A. 2009; 15:2227–2236. [PubMed: 19207036]
15. Mauney JR, Nguyen T, Gillen K, Kirker-Head C, Gimble JM, Kaplan DL. Engineering adipose-like tissue in vitro and in vivo utilizing human bone marrow and adipose-derived mesenchymal stem cells with silk fibroin 3D scaffolds. Biomaterials. 2007; 28:5280–5290. [PubMed: 17765303]
16. Wang Y, Rudym DD, Walsh A, Abrahamsen L, Kim H-J, Kirker-Head C, et al. In vivo degradation of three-dimensional silk fibroin scaffolds. Biomaterials. 2008; 29:3415–3428. [PubMed: 18502501]
17. Rockwood DN, Preda RC, Yücel T, Wang X, Lovett ML, Kaplan DL. Materials fabrication from Bombyx mori silk fibroin. Nat Protoc. 2011; 6:1612–1631. [PubMed: 21959241]
18. Choi JH, Bellas E, Vunjak-Novakovic G, Kaplan DL. Adipogenic differentiation of human adipose-derived stem cells on 3D silk scaffolds. Methods Mol Biol. 2011; 702:319–330. [PubMed: 21082412]
19. Yoshimura K, Shigeura T, Matsumoto D, Sato T, Takaki Y, Aiba-Kojima E, et al. Characterization of freshly isolated and cultured cells derived from the fatty and fluid portions of liposuction aspirates. J Cell Physiol. 2006; 208:64–76. [PubMed: 16557516]
20. Pallua N, Pulsfort AK, Suschek C, Wolter TP. Content of the growth factors bFGF, IGF-1, VEGF, and PDGF-BB in freshly harvested lipoaspirate after centrifugation and incubation. Plast Reconstr Surg. 2009; 123:826–833. [PubMed: 19319045]
21. Numata K, Cebe P, Kaplan DL. Mechanism of enzymatic degradation of betasheet crystals. Biomaterials. 2010; 31:2926–2933. [PubMed: 20044136]
22. Takemura R, Werb Z. Secretory products of macrophages and their physiological functions. Am J Physiol. 1984; 246:C1–C9. [PubMed: 6364825]
23. Rubin JP, DeFail A, Rajendran N, Marra KG. Encapsulation of adipogenic factors to promote differentiation of adipose-derived stem cells. J Drug Target. 2009; 17:207–215. [PubMed: 19558360]
24. Kim U-J, Park J, Kim HJ, Wada M, Kaplan DL. Three-dimensional aqueousderived biomaterial scaffolds from silk fibroin. Biomaterials. 2005; 26:2775–2785. [PubMed: 15585282]
25. Angele P, Abke J, Kujat R, Faltermeier H, Schumann D, Nerlich M, et al. Influence of different collagen species on physico-chemical properties of crosslinked collagen matrices. Biomaterials. 2004; 25:2831–2841. [PubMed: 14962561]
26. Park YD, Tirelli N, Hubbell J. Photopolymerized hyaluronic acid-based hydrogels and interpenetrating networks. Biomaterials. 2003; 24:893–900. [PubMed: 12504509]
27. Kilroy GE, Foster SJ, Wu X, Ruiz J, Sherwood S, Heifetz A, et al. Cytokine pro.le of human adipose-derived stem cells: expression of angiogenic, hematopoietic, and pro-in.ammatory factors. J Cell Physiol. 2007; 212:702–709. [PubMed: 17477371]
28. Zannettino AC, Paton S, Arthur A, Khor F, Itescu S, Gimble JM, et al. Multipotential human adipose-derived stromal stem cells exhibit a perivascular phenotype in vitro and in vivo. J Cell Physiol. 2008; 214:413–421. [PubMed: 17654479]

NIH-PA Author Manuscript
NIH-PA Author Manuscript
NIH-PA Author Manuscript

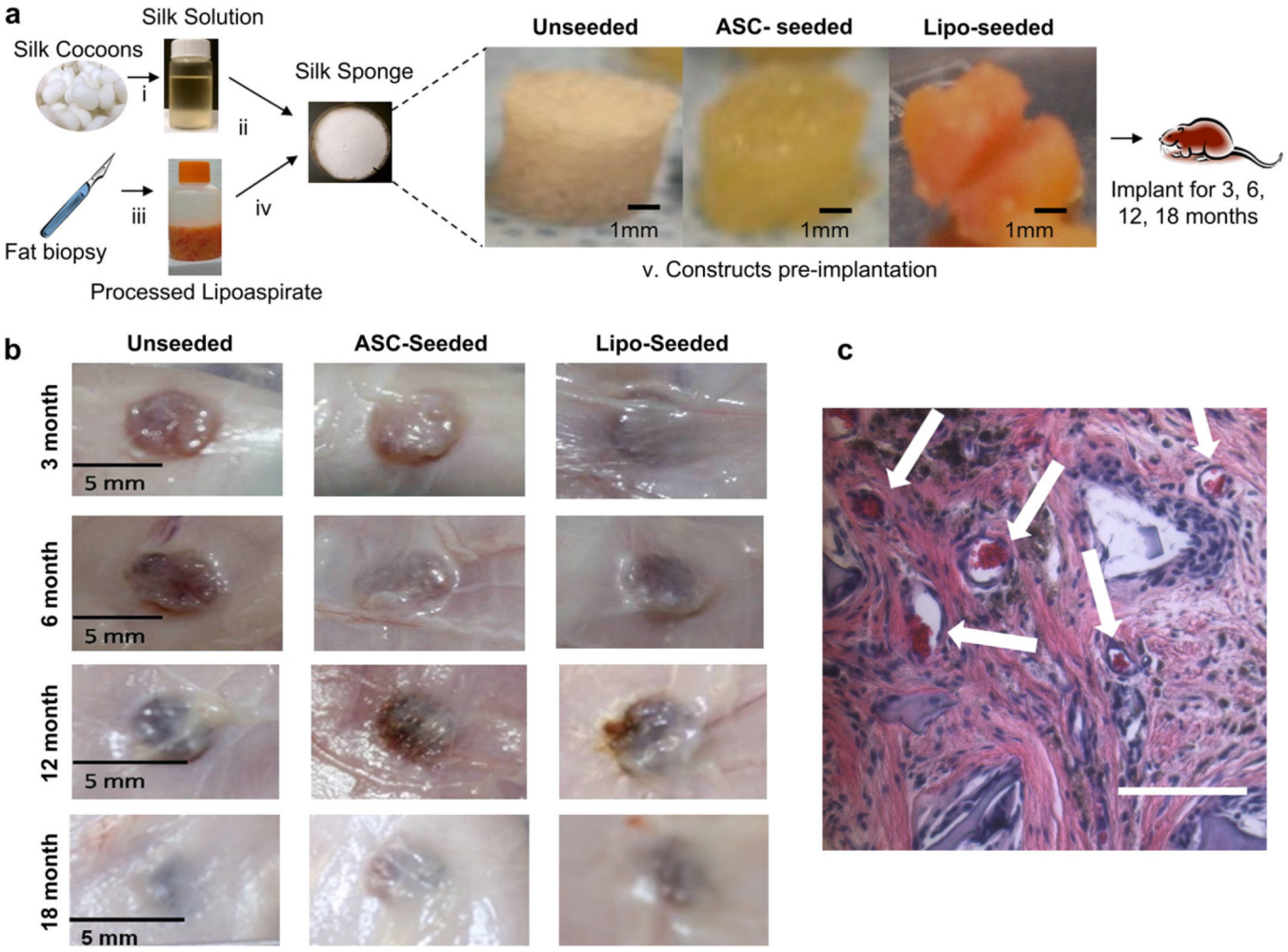

Fig. 1.

Clinically translatable process for soft tissue regeneration. (a) Porous silk sponges were prepared as described in Methods (i). The aqueous solution was lyophilized, re-dissolved in an organic solvent, and cast into a porous sponge format using a salt-leaching method (ii), cut to the desired dimensions and autoclaved. No further processing was required for unseeded groups. The seeded groups were prepared by first obtaining lipoaspirate, and clearing the fat of free oils and blood (iii). For the ASC-seeded group, ASCs were isolated by a collagenase digestion followed by an adherence selection process. ASCs were seeded onto the silk sponges and cultured for 1 month under adipogenic conditions (iv) prior to implantation. For the lipo-seeded group, the silk sponges were soaked in the processed lipoaspirate for 1 h (iv) prior to implantation. Macroscopic images of unseeded (left), ASC-seeded (middle) and lipo-seeded (right) constructs prior to implantation (v). The constructs were implanted subcutaneously in the dorsal region of a nude rat for 3, 6, 12 and 18 months. (b) Macroscopic images of constructs after 3 (top row), 6 (second row), 12 (third row) and 18 (bottom row) months *in vivo*, prior to being explanted. Integration with the surrounding host tissue increased when the silk sponges were pre-seeded. By 12 months, all groups were similarly integrated. (c) Functional blood vessels support regenerating tissue. H&E image of unseeded group at 6 months show functional blood vessels containing red blood cells (white arrows). The vasculature is a result of ingrowth from the host. Scale bar – 100 μm. (For interpretation of the references to color in this figure legend, the reader is referred to the web version of this article.)

NIH-PA Author Manuscript
NIH-PA Author Manuscript
NIH-PA Author Manuscript

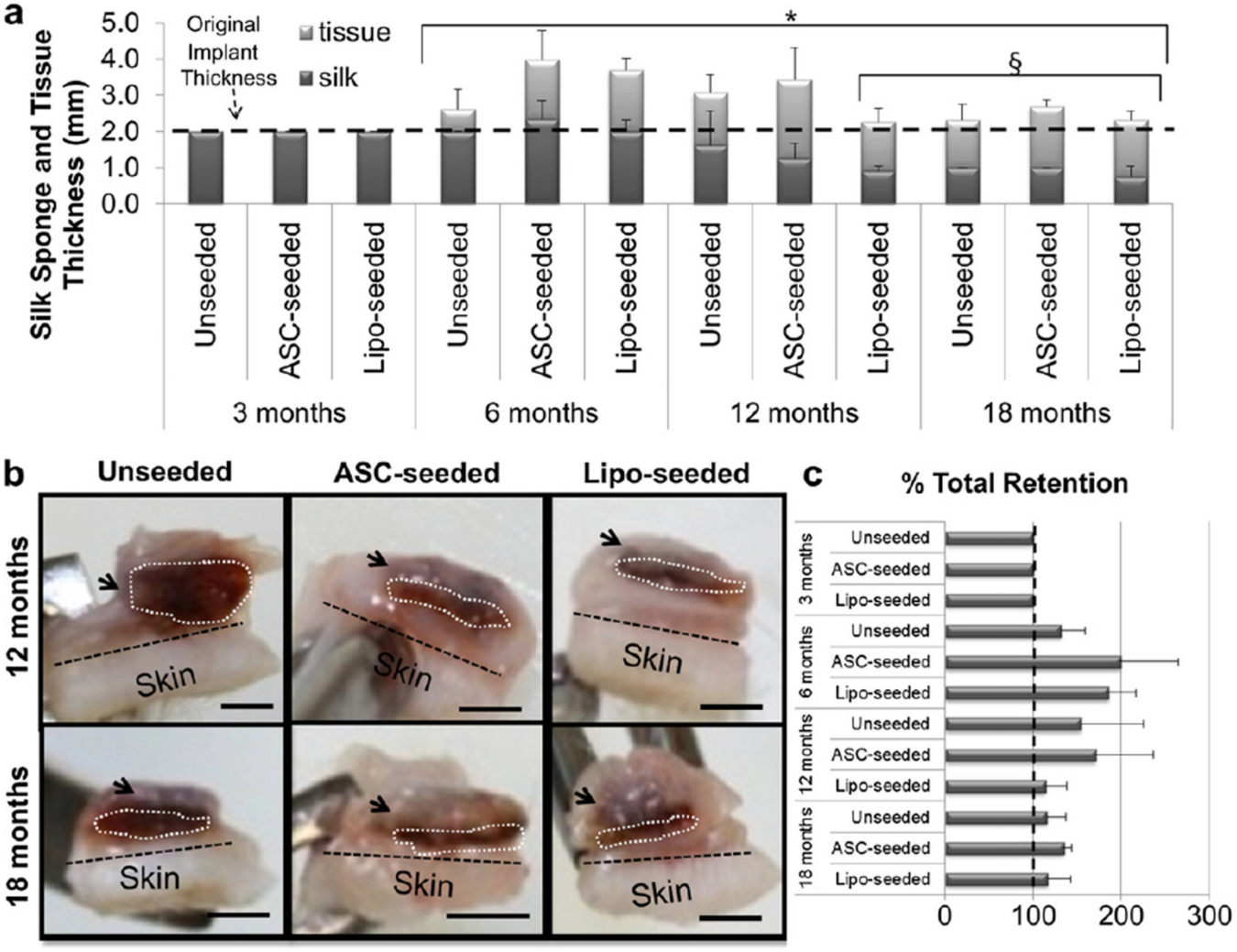

Fig. 2.

Tissue regeneration occurs with silk sponge degradation. (a) The silk sponge volume was calculated by measuring the silk sponge thickness and diameter upon explantation. The volume was maintained, i.e. no biomaterial degradation, through 6 months. At 12 and 18 months, the seeded groups degraded more quickly than the unseeded group. Tissue thickness had significantly increased at 6, 12 and 18 months when compared to 3 months (* indicates $p < 0.0001$). Sponge size had significantly decreased at 12 months for the lipo-seeded group, and at 18 months for all groups (§ indicates $p < 0.05$). (b) Cross-sections of 12 (top) and 18 (bottom) month explants are shown for unseeded (left), ASC-seeded (middle) and lipo-seeded (right) groups. The region in the white dotted line outlines the silk sponge, while the black dotted line demarcates the skin from the subcutaneous tissue. The arrows point to regions of subcutaneous fat. The subcutaneous fat formation was greatest in the lipo-seeded group (right column) and least in the unseeded group (left column). Scale bar – 2 mm. (c) Approximated thickness of the newly formed tissue was determined by measuring the thickness of the fat and subtracting the thickness of the silk sponge by image analysis in ImageJ. There were no statistically significant changes in total % retention.

NIH-PA Author Manuscript
NIH-PA Author Manuscript
NIH-PA Author Manuscript

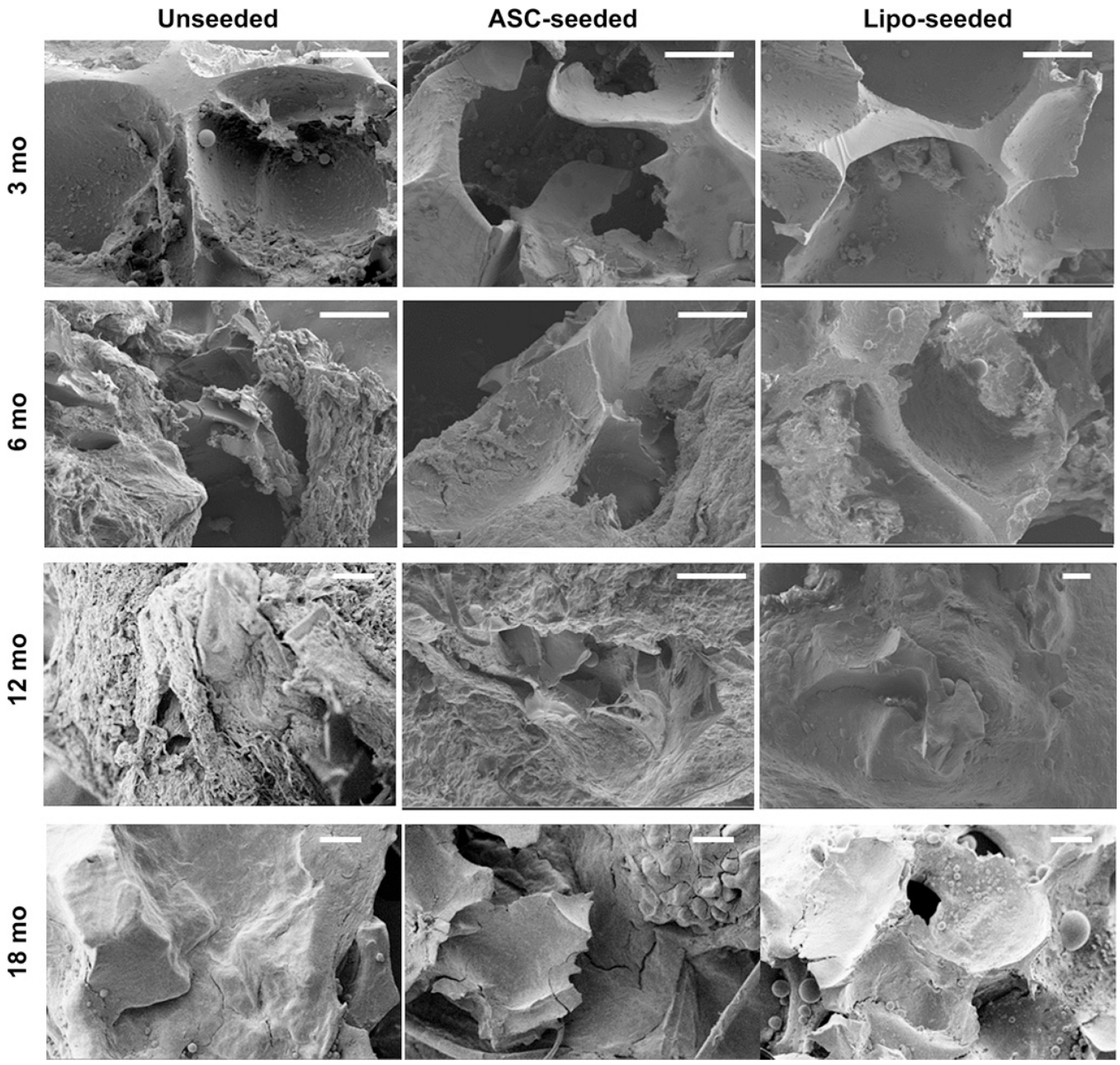

Fig. 3.

Silk sponge pore wall thickness did not change over time. Silk sponge pores were observed by SEM. No differences in thickness were seen over time which confirmed our observation that degradation occurred from outer part of the sponge inwards. The ranges of pore wall thickness were determined by image analysis in SmartTiff (Carl Zeiss Microscopy). Average pore wall thicknesses ranged from ~ 10 to 40 μm. The overall sponge structure remained intact with open pores and tissue infiltration. Each pore wall was measured 3 times, and each sample was measured in 8 different locations per image. Scale bar – 100 μm.

NIH-PA Author Manuscript
NIH-PA Author Manuscript
NIH-PA Author Manuscript

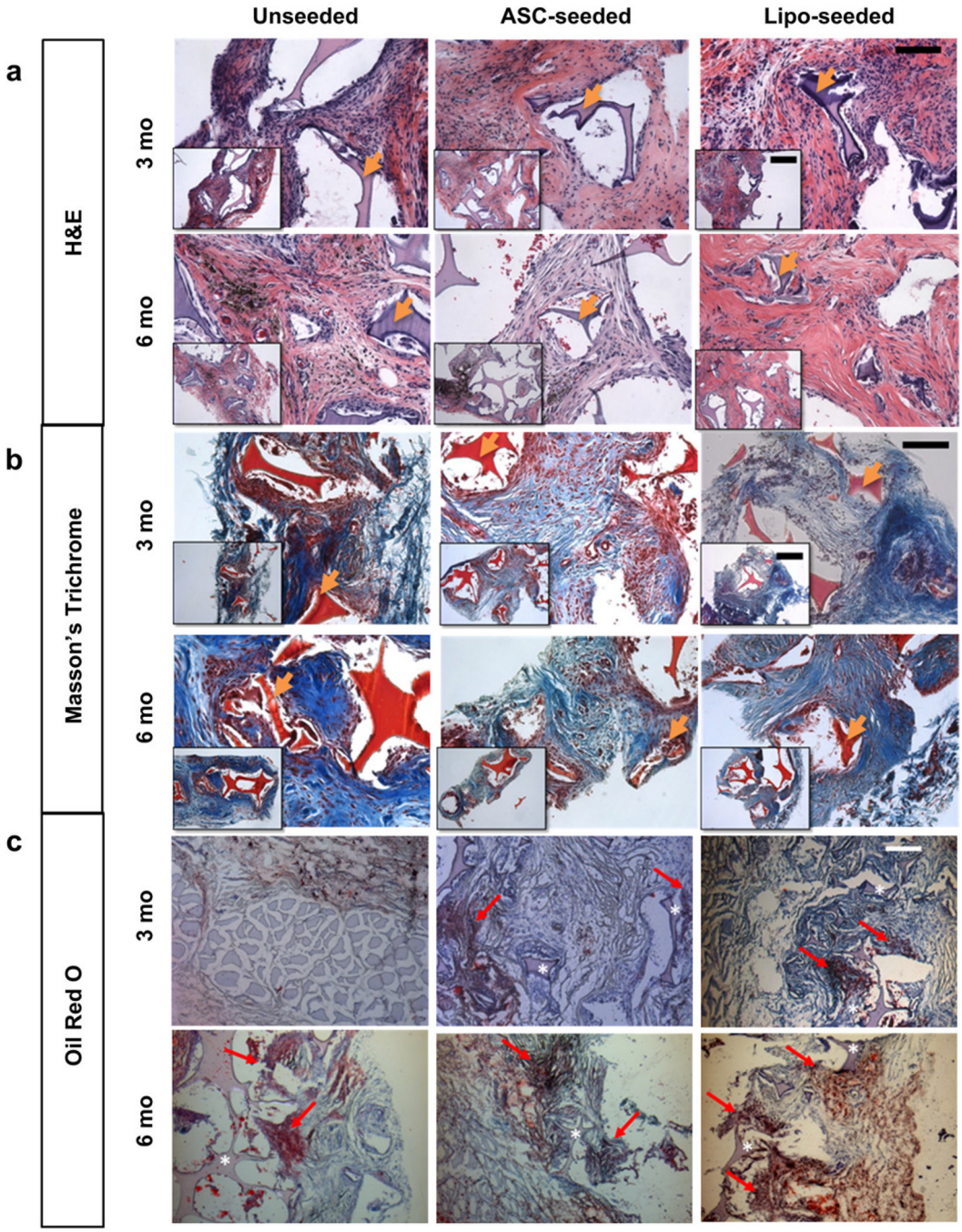

Fig. 4.

Histological tracking of regenerated tissue show an active tissue remodeling process. (a) H&E images at 3 (top) and 6 months (bottom) show a decrease in macrophages within the sponge from 3 to 6 months. Macrophages are seen surrounding the silk pore wall in the unseeded group (left) at 3 and 6 months. The intact silk sponge stains a dark purple and is visible in all groups. Hemosiderin deposits (dark or black deposits) were present is some sections as with the later timepoints (see Supplementary Fig. 2). Scale bar – 100 μm, inset – 200 μm. (b) Masson's Trichrome staining for tissue organization at 3 (top) and 6 months (bottom). The intact silk sponge stains red and is visible in all groups. At 3 months, the unseeded study group (left) has a collagenous matrix (blue) that is poorly organized in

NIH-PA Author Manuscript

NIH-PA Author Manuscript

NIH-PA Author Manuscript

comparison to the seeded groups. By 6 months (bottom) more matrix (blue) is seen. Scale bar – 100 μm, inset – 200 μm. (c) Oil Red O (ORO) for staining mature adipocytes at 3 (top) and 6 months (bottom). The intact silk sponge (asterisk) stains a light purple and is visible in all groups. Areas of ORO positive staining are pointed to with a red arrow. At 3 months (top), only the seeded groups (middle, right) were positive for ORO, the unseeded group (left) was positive for ORO only near the underlying muscle as shown. The lipo-seeded group (right) stained the most densely for ORO. Scale bar – 200 μm. (For interpretation of the references to color in this figure legend, the reader is referred to the web version of this article.)

NIH-PA Author Manuscript
NIH-PA Author Manuscript
NIH-PA Author Manuscript

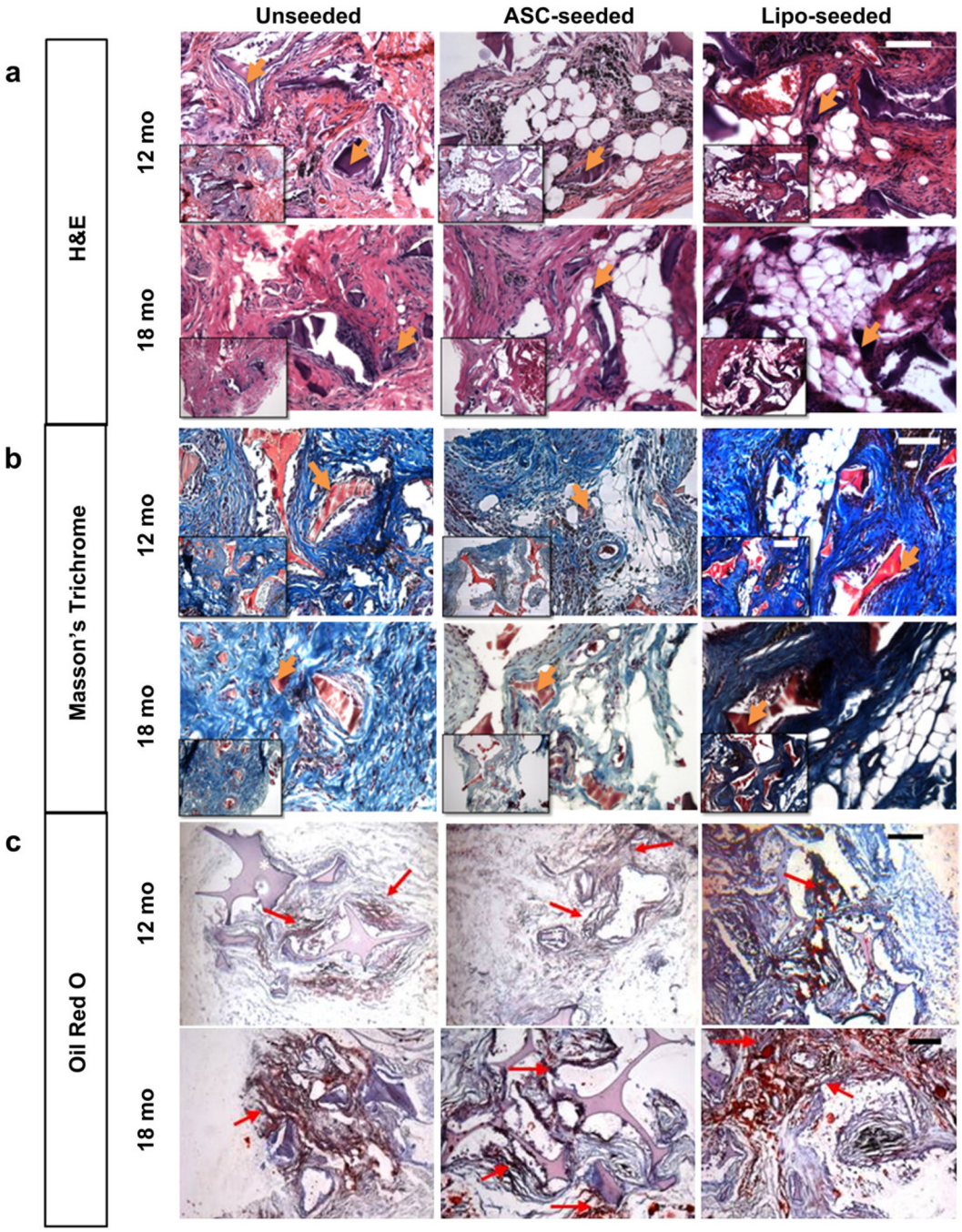

Fig. 5.

Histological tracking of regenerated tissue shows mature adipocytes/fat formation in seeded groups at 12 and 18 months. (a) H&E images at 12 (top) and 18 months (bottom) show that fat formation was present in seeded groups. The silk sponge stains a dark purple and is visible in all groups. At 12 months, the silk sponge walls began to fracture as the sponge degraded. In some sections, dark, or black deposits of hemosiderin were seen (see Supplementary Fig. 2). Scale bar – 100 μm, inset – 200 μm. (b) Masson's Trichrome staining for tissue organization at 12 (top) and 18 months (bottom). The silk sponge stains red and is visible in all groups. The cellularity (nuclei stain dark or black), decreased from 12 to 18 months in all groups, and then is replaced with a well-organized collagenous matrix

NIH-PA Author Manuscript

NIH-PA Author Manuscript

NIH-PA Author Manuscript

(blue). Scale bar – 100 μm, inset – 200 μm. (c) Oil Red O (ORO) for staining mature adipocytes at 12 (top) and 18 months (bottom). The silk sponge (asterisk) stains a light purple and is visible in all groups. Areas of ORO positive staining are pointed to with a red arrow. The lipo-seeded groups (right) stained the most densely for ORO. Scale bar – 200 μm. (For interpretation of the references to color in this figure legend, the reader is referred to the web version of this article.)

NIH-PA Author Manuscript
NIH-PA Author Manuscript
NIH-PA Author Manuscript

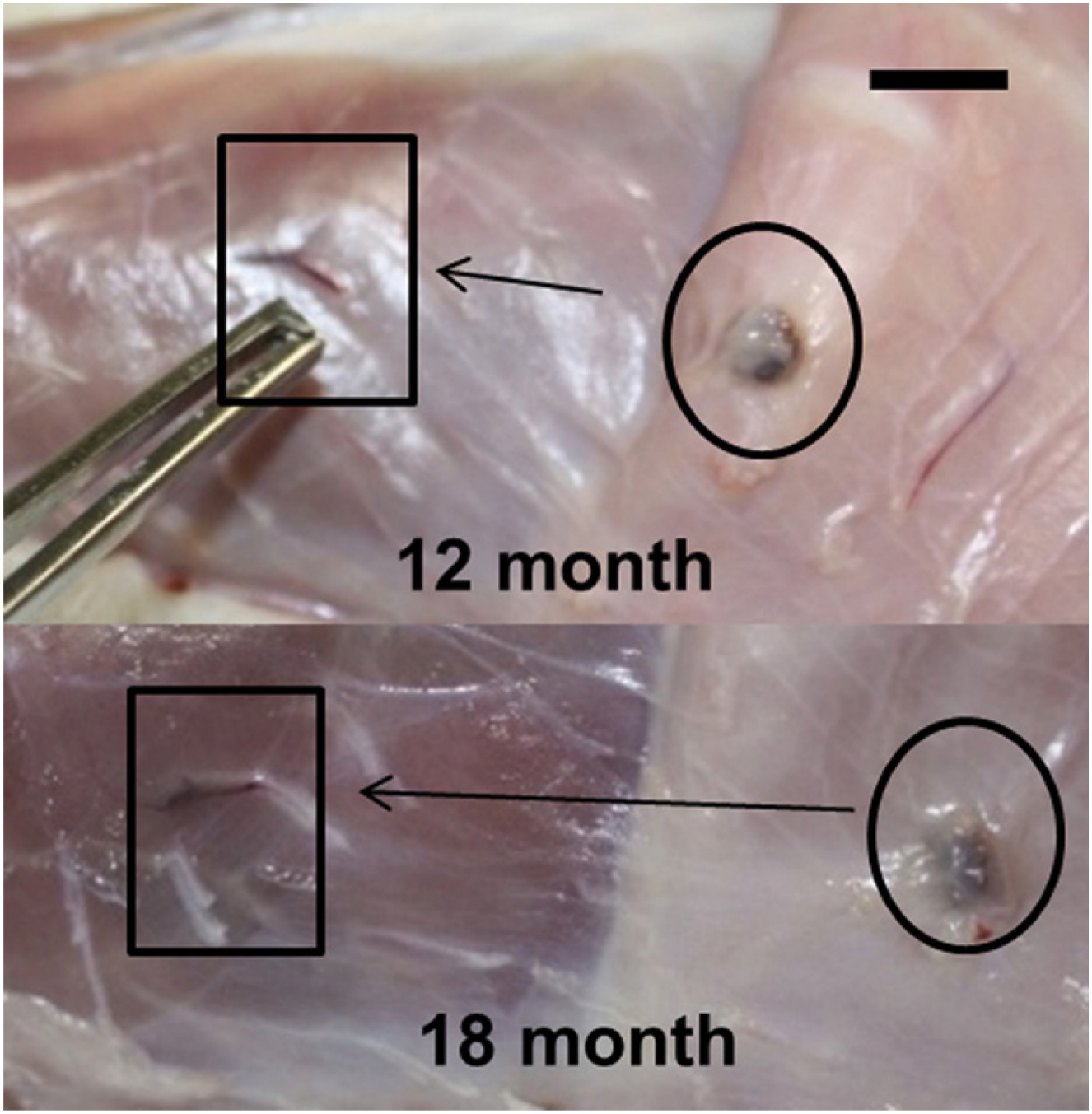

Fig. 6.
At 12 and 18 months in the lipo-seeded group, a large vessel was found feeding into the lipo-seeded construct from the underlying muscle. This was not seen at earlier timepoints or in other groups. Scale bar – 1 mm.